ACS Catalysis

Letter

pubs.acs.org/acscatalysis

High Alcohols Synthesis via Fischer−Tropsch Reaction at Cobalt Metal/Carbide Interface

Yan-Peng Pei,[†,∥] Jin-Xun Liu,[‡,∥] Yong-Hui Zhao,[‡] Yun-Jie Ding,[*,†,‡] Tao Liu,[†] Wen-Da Dong,[†] He-Jun Zhu,[†] Hai-Yan Su,[‡] Li Yan,[†] Jin-Lin Li,[§] and Wei-Xue Li[*,‡]

[†]Dalian National Laboratory for Clean Energy, Dalian Institute of Chemical Physics, Chinese Academy of Sciences, Dalian 116023, China

[‡]State Key Laboratory of Catalysis, Dalian Institute of Chemical Physics, Chinese Academy of Sciences, Dalian 116023, China

[§]Key Laboratory of Catalysis and Materials Science of the State Ethnic Affairs Commission & Ministry of Education, South-Central University of Nationalities, Wuhan 430074 China

Supporting Information

ABSTRACT: Utilization of nonprecious transition metals for high alcohols synthesis is of a great importance in heterogeneous catalysis. We synthesized successfully cobalt metal-carbide (Co−Co_2C) catalysts, which present remarkable activity and selectivity for high alpha-alcohols via the Fischer−Tropsch reaction. The formation of the stable cobalt carbide and the Co−Co_2C interface are found to be essential for the observed reactivity. Density functional theory calculations show that Co_2C is highly efficient for CO nondissociative adsorption, behaving as noble-metal-like, whereas the Co metal is highly active for CO dissociative adsorption and the subsequent carbon-chain growth. The interface between the cobalt metal and its carbide phase, as well as the dual sites available at the interface for facile CO insertion to hydrocarbon, could be used to rationalize the design of the nonprecious transition metal catalysts for the oxygenates in syngas conversion.

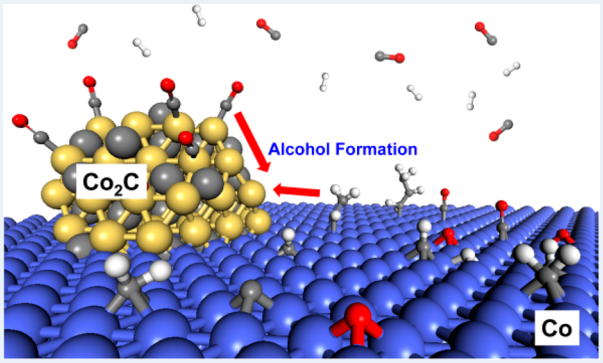

KEYWORDS: *high alcohols synthesis, Fischer−Tropsch reaction, interface, cobalt, carbide*

The high alcohol ($C_nH_{2n+1}OH$, $n \geq 6$) synthesis (HAS) is an important process in basic chemical industries, and the products are used widely as feedstock of plasticizers, detergents, and lubricants. HAS is traditionally produced by a multistep ALFOL alcohol process[1] including hydrogenation, ethylation, growth reaction, oxidation, and hydrolysis. HAS can also be produced by the hydroformylation[2−5] of a mixture of olefins and H_2/CO by homogeneous precious metal catalysts, which negatively impacts the separation of products. Alternatively, homogeneous catalysts were used for hydroformylation and subsequent hydrogenation of alpha-olefins from Fischer−Tropsch (F−T) synthesis, and this would unfortunately form not only alpha-alcohols but also undesired branched alcohols.[2,6,7] It is therefore highly valuable to find a one-step synthesis technique and nonprecious metal catalysts that could directly produce high alcohols with low selectivity of light alkanes and methanol.

We found in the past a one-step synthesis of aliphatic C_1−C_{18} alpha-alcohols with high-quality fuels and low methanol from syngas via F−T reaction using nonprecious cobalt catalysts supported on an activated carbon.[8,9] The prepared catalysts were promising and exhibited excellent stability for more than 2000 h. In all spent catalysts, the formation of cobalt carbide (Co_2C) was observed.[10,11] Actually, the formation of cobalt carbide and influence in higher alcohol synthesis was reported earlier by Mausbeck et al.,[12] Zaikovskii et al.,[13] and later by Wang et al.[14] This indicated that the formation of Co_2C might be responsible for the direct synthesis of the high alpha-alcohols. This is surprising because in F−T synthesis, Co_2C had a rather low activity,[15] and its formation was often regarded as a sign of the catalyst deactivation.[16−20] On the other hand, the metal carbide was well-known for its noble-metal-like feature and could catalyze various reactions such as hydrogenation,[21] desulfurization,[22] and the water-gas shift reaction.[23] Resolving this controversy is however prevented by the influence of the supports and promoters often involved in the catalysts. The formation and stability of cobalt carbide was also sensitive to the support, pretreatment, and reaction condition.

We synthesized here successfully stable and efficient Co−Co_2C catalysts for high alcohol via the F−T reaction, free from the supports and promoters. The formation of the Co and Co_2C interface and the dual sites at the interface were found essential for efficient alcohol synthesis via the F−T reaction.

Received: January 21, 2015
Published: May 11, 2015

DOI: 10.1021/acscatal.5b00791
ACS Catal. 2015, 5, 3620−3624

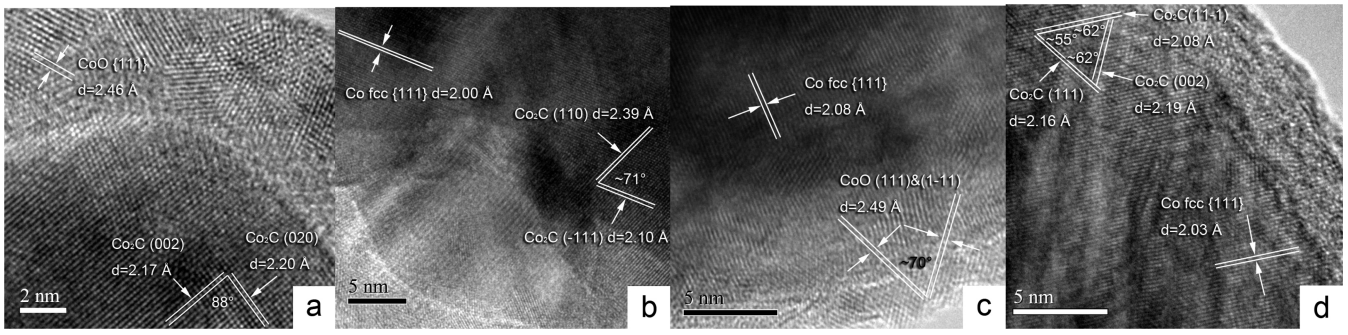

Figure 1. HRTEM images of the Co−Co_2C, Co−Co_2C/AC1, and Co/AC2 catalysts: (a) as-prepared Co_2C sample; (b) the spent Co−Co_2C catalyst; (c) the spent Co/AC2 catalyst; (d) the spent Co−Co_2C/AC1 catalyst after F−T reaction.

Density functional theory calculations found that Co_2C provides the active sites for CO nondissociative adsorption, and the Co metal provides the active sites for CO dissociative adsorption and subsequent carbon-chain growth; the CO insertion to hydrocarbon for oxygenates at the Co and Co_2C interface is facile.

To reveal the intrinsic activity of cobalt carbide free of influence of the supports and promoters, we synthesized the unsupported and pure Co_2C according to Bahr and Jessen's method.[24] In this method, Co_3O_4 was fully reduced first in H_2 at 553 K and subject to an extensive carburization by CO at 493 K for at least 468 h. The good crystallinity of Co_2C as prepared can be justified from the clear lattice fringe of 2.17 and 2.20 Å in the HRTEM image (Figure 1a and Table S1), which are characteristic interlayer spacing of Co_2C (002) and (020) planes. The lattice fringe of 2.46 Å on top of Co_2C substrate comes from the oxide passivation layer CoO(111). In situ XRD measurement (Figure 2) gives the peaks at 2θ = 37.0, 41.3, 42.6, 45.8, and 56.6°, which can be assigned to the crystalline plane of Co_2C (110), (002), (111), (021), and (112) according to PDF 01-072-1369, respectively. No peaks from the Co metal can be observed. The as-prepared Co_2C is stable in a H_2 flow until 423 K, as seen from in situ XRD measurement. It starts to decompose into fcc and hcp Co at higher temperature, and the decomposition rate reaches a maximum between 473 and 523 K, consistent with previous results.[15,17] The characteristic Co_2C peaks disappears completely when temperature is higher than 573 K.

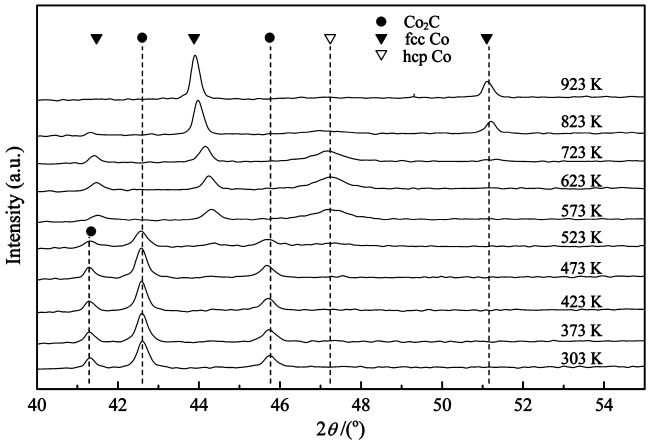

Figure 2. In situ XRD pattern for the unsupported bulk Co_2C sample in a H_2 flow during temperature-programmed reaction.

The as-prepared Co_2C catalysts were tested for the F−T reaction under a typical condition of 493 K, 3.0 MPa, H_2/CO molar ratio of 2, and 33.6 mL·min^{-1} (Figure S1). Though the corresponding temperature is high enough to decompose the cobalt carbide as indicated above, the presence of CO would however stabilize the corresponding carbide and prevent its complete decomposition.

This is indeed verified by the high-resolution transmission electron microscopy (HRTEM) image of the spent Co_2C sample after the F−T reaction and X-ray diffraction measurement (Figure S2). As shown in Figure1b, the lattice fringe of 2.00 Å from the Co metal (not present before the reaction in Figure1a) is clearly seen, whereas the lattice fringe of 2.10 and 2.39 Å from Co_2C remains. Namely, as-prepared Co_2C was only partially decomposed to the Co metal, and both coexist under the F−T reaction condition. Because Co metal comes from the decomposition of Co_2C, naturally, there is considerable interface between Co and Co_2C (noted as Co−Co_2C hereafter) formed, as seen evidently in the HRTEM image. As shown later, the presence of Co_2C and its interface with the Co metal is essential for the efficient high alcohol selectivity.

The reactivity of Co−Co_2C catalysts generated during the F−T reaction is summarized in Table 1. The linear alpha-alcohols (C_1−C_{18}), naphtha distillates, and diesel fuels are all possible products through F−T reaction. The CO conversion is

Table 1. Evaluation Results of CO Hydrogenation over the Unsupported Co−Co_2C, Co−Co_2C/AC1, and Co/AC2 Catalysts[a]

	BET[b]		selectivity (C %)					alcohol distribution (C %)		
catalyst	SA, m^2/g	CO con%	C_1−C_4	CO_2	C_{5+}	alcohols	others	C_1OH	C_2−C_5OH	C_6−$C_{18}OH$
Co−Co_2C	8.7	25.3	32.4	4.6	26.0	37.0	1.4	13.0	60.9	26.1
Co−Co_2C/AC1	683	71.4	20.8	5.1	35.7	38.4	0.0	8.4	52.5	39.1
Co/AC2	648	55.5	31.5	7.6	53.4	7.5	0.0	14.2	40.2	45.6

[a]Reaction conditions: H_2/CO = 2.0, temperature 493 K, pressure 3.0 MPa, total flow rate 33.6 mL·min^{-1}; FT reactions were tested on the basis of almost the same total Co loading of three catalysts. [b]The surface areas of AC1 and AC2 were 1135 and 1068 m^2/g, respectively. The other texture and structural properties of AC1 and AC2 were almost the same.

DOI: 10.1021/acscatal.5b00791
ACS Catal. 2015, 5, 3620−3624

25.3%, the selectivities of light hydrocarbons (C_1-C_4) and CO_2 are only 32.4 and 4.6%, and the alcohol selectivity is as high as of 37.0%. The alcohol and hydrocarbon distributions on the Co−Co_2C were in good agreement with Anderson−Schulz−Flory (ASF) distribution. Importantly, among the alcohols produced, the distributions from ethanol, C_2-C_5 linear alpha-alcohols, and C_6-C_{18} linear alpha-alcohols were 13.0, 60.9 and 26.1%, respectively. The selectivity of the high linear alpha-alcohol is significant. Because there is no support and promoter in this catalyst, this result shows that the corresponding activity and selectivity comes solely from Co−Co_2C.

To prepare the supported Co−Co_2C catalysts with high dispersion, it is challenging to find the proper supports which could easily form Co_2C species. We achieved this on a unique activated carbon (AC1) from a coconut shell. Using this support, the dispersed Co catalysts can be carburized to a significant amount of Co_2C in a flow of syngas, as seen from XRD (Figure S5). The reactivity of the as-prepared catalysts (noted as Co−Co_2C/AC1) under the same F−T reaction conditions used above is given in Table 1. Similar to the unsupported Co−Co_2C, a rather high linear alpha-alcohol selectivity of 38.4% was obtained. The alcohol and hydrocarbon distributions on the Co−Co_2C/AC1 were also in good agreement of ASF distribution, respectively, as the unsupported one. The difference with respect to the unsupported one was that the distribution of high alpha-alcohols (C_6^+) increased from 26.1% up to 39.1% in total alcohols. Moreover, the CO conversion increased dramatically from 25.1% to 71.4% due to the increase of cobalt component dispersion and surface area. Figure 1d shows the corresponding HRTEM image after the F−T reaction. The lattice fringe of 2.16, 2.19, and 2.08 Å from Co_2C (111), (002), and (11−1) planes and that of 2.03 Å from the fcc Co(111) plane in direct contact with the former one to form Co−Co_2C interfaces are clearly seen. XRD measurement (Figure S3 in SI) also confirms the coexistence of Co and Co_2C phases, fully consistent with the unsupported Co−Co_2C.

To see the possible role of Co_2C more clearly, a Co catalyst supported on an activated carbon from an almond nut and pretreated by an aqueous diluted HCl was prepared. The catalyst was reduced in hydrogen, and there is no presence of Co_2C observed after carburization in a flow of syngas from XRD in Figure S4. The prepared catalyst (noted as Co/AC2) was test for the F−T reaction, and the corresponding reactivity is given in Table 1.Though the CO conversion is as high as 55.5%, which is inline with its higher surface area, the main product is the hydrocarbons with selectivity of 84.9%, and the alcohol selectivity (7.5%) is rather low. This is a typical result found in supported cobalt catalysts for F−T synthesis.[25,26] The HRTEM image of the spent Co/AC2 (Figure1c) shows that the catalyst composes mainly the fcc Co with the lattice fringe of of 2.08 Å from Co(111), in addition of the oxide passivation layer with the lattice fringe of 2.49 Å from CoO(111). Importantly, Co_2C is hardly seen for Co/AC2 catalyst even after the F−T reaction.

The above results show that the presence of Co_2C dramatically increases the alcohol selectivity. Further experiments at similar CO conversion by varying flow rate (Table S2) also show similar activity and selectivity. Moreover, by adding different structure promoters such as La and Zr, the relative ratio of Co_2C and Co could be changed. As seen from Figure S6, with a higher ratio of Co_2C/Co, there is a higher alcohol selectvity. Because neither Co_2C nor Co alone could achieve the high reactivity of alcohol observed, independent of the flow rate, it is thus the formed Co_2C and Co interface that is responsible for the observed reactivity in both supported and unsupported Co−Co_2C catalysts.

In terms of the underlying reaction mechanism, we first note the following: the fact only alpha-alcohols are produced on both supported and unsupported Co−Co_2C catalysts dictates that the formation of alcohols via the hydroformylation of the olefin intermediates from F−T reaction with a CO/H_2 can be excluded, because otherwise, it would produce branch-alcohols. Moreover, the alcohol and hydrocarbon distributions on Co−Co_2C catalysts, as found similarly in our earlier result,[10] follows the ASF distribution. Because the F−T reaction on pure Co metal catalysts follows ASF distribution as well, the similar ASF distribution found on Co−Co_2C implies that the chain propagation on the Co−Co_2C catalysts may occur mainly on the Co metal part, providing the active sites for which CO dissociates and hydrogenates to form CH_x monomer, initiating the chain growth through C−C coupling.[27−29] This is likely because the Co metal catalyst is well documented in the literature for its high selectivity of the linear hydrocarbon in the F−T reaction,[26,30] and this also corroborates the present findings of only linear alcohol formed on Co−Co_2C catalysts. The essence of Co_2C in Co−Co_2C catalysts could be therefore rationalized by providing the active sites for CO nondissociative adsorption, coupling with the linear hydrocarbon intermediates formed on the Co metal part at the Co and Co_2C interfaces to form linear oxygenates, which are subject to further hydrogenation to selectively produce the linear alpha-alcohols.

Metal carbides are usually less reactive than the corresponding metal and noble-metal-like phases,[31,32] and the nondissociative adsorption of CO molecules on Co_2C is possible. To shed further light on this, we resort to DFT calculations (details in SI) on CO adsorption and dissociation. Co_2C has an orthorhombic structure, and the Co−Co distances in bulk Co_2C (2.61 and 2.87 Å) are 5% ∼ 15% larger than those (2.49 Å) in the Co metal. Calculated density of states (Figure S7 and S8) shows that Co_2C is metallic in nature: Co is a cation with a Bader charge of 0.48 *e*, and C is anion with Bader charge of about −0.99 *e*. The distinct geometrical and electronic features of Co_2C from the Co metal have great impact on the corresponding reactivity, as seen below.

According to the above experiments and previous DFT study,[33] two representative Co_2C (111) and (110) surfaces with lower surface energy were considered, and an open fcc Co(100) surface was also calculated for reference. The Co-terminated Co_2C surfaces representing the structure under H-rich condition (lower CO/H_2 ratio) was first studied. Compared to the binding energy of CO* (−1.71 eV) at the favorable 4-fold site of Co(100) (Figure 3e), the binding energy of CO* (−2.21 eV) at the favorable 3-fold site of Co_2C(111) (Figure 3b) is enhanced by almost 0.50 eV. The origin for this comes from the lattice expansion and positive charge of Co in Co_2C. In particular, for the latter one, the positive charge of Co greatly facilitates σ-donation from CO*, strengthening its chemical bonding with Co cation underneath. On the other hand, the positive charge Co in Co_2C is energetically unfavorable for binding the highly electronegative species, such as atomic C and O. The limited charge transfer from Co cation to C* and O* as well as their electrostatic repulsion with lattice C in Co_2C would destabilize the overall energetic. Actually, for C*, the calculated binding strength (−7.74 eV) at the most favorable site of Co_2C (111) (Figure 3d) is weakened by 0.27 eV than that of Co(100) (−8.01 eV, Figure 3g),

DOI: 10.1021/acscatal.5b00791
ACS Catal. 2015, 5, 3620−3624

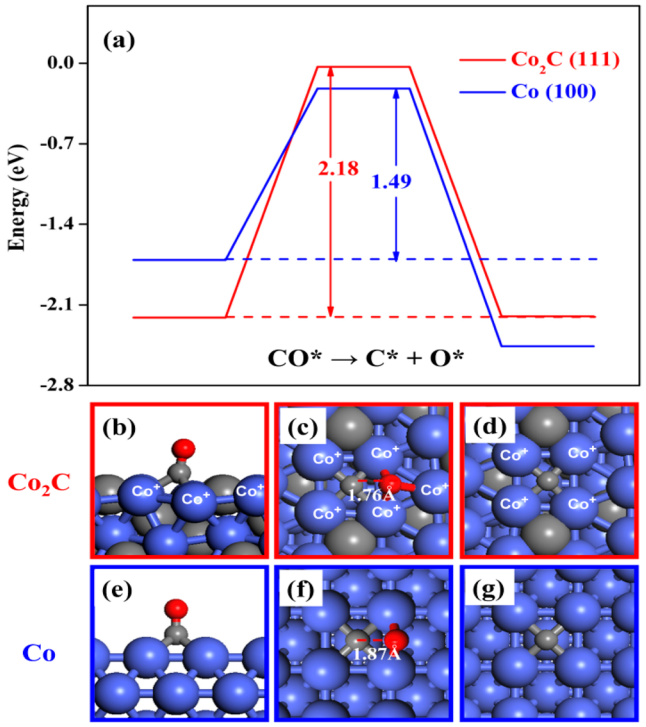

Figure 3. Energetic and geometric information for direct CO activation on Co_2C (111) (red) and fcc Co (100) (blue) surfaces: (a) potential energy diagram for direct CO dissociation (activation barriers and reaction energies in eV are indicated). (b), (c), and (d) are CO adsorption, CO dissociation transition state, and atomic C adsorption on Co_2C (111), while (e), (f), and (g) are those on Co (100) surface.

whereas for O*, the corresponding binding strength is similar (−5.99 eV) on both surfaces (Table S3).

Stabilizing the CO* molecule but destabilizing the C* species on Co_2C have a great impact on reaction energetics and kinetics for CO dissociation. For instance, the calculated reaction energy for direct dissociation CO* to C* and O* on $Co_2C(111)$ is thermal neutral (0.01 eV), whereas it is highly exothermic (−0.75 eV) on Co(100) (Table S4). Because the corresponding transition states on two surfaces (Figure 3c,f) are similar, the dramatic decrease of the reaction energy on $Co_2C(111)$ would suppress the corresponding kinetics. The calculated barrier of 2.18 eV is indeed much higher than that of 1.49 eV on Co(100), as plotted in Figure 3a. Under the F−T reaction condition, CO activation may be assisted by the presence of hydrogen, which is particularly true for the catalysts with relative lower activity.[34,35] We also tested this reaction pathway, and the calculated effective barrier for CO*+H*→ HCO*→ CH*+O* on $Co_2C(111)$ is 2.12 eV, just 0.06 eV lower than that of the direct pathway (Figure S9). Whereas on Co(100), the corresponding barrier of 1.52 eV for the H-assisted pathway remains modest. Considering the F−T reaction temperature (493 K), the barriers on $Co_2C(111)$ are too high to dissociate CO efficiently. In other words, $Co_2C(111)$ could provide the efficient sites for nondissociative adsorption of CO molecules, behaving as noble-metal-like.

The above conclusion applies also for different Co_2C surfaces and CO/H_2 ratio (Table S5, S6, Figure S10, S11, S12, and S13). On the Co-terminated $Co_2C(110)$ surface,the calculated CO binding energy is −2.01 eV, and the corresponding dissociation barriers are 2.16 and 1.86 eV for direct and H-assisted pathway (Figure 4), respectively. Under higher CO/H_2 ratio condition (carbon rich), C-terminated Co_2C surfaces

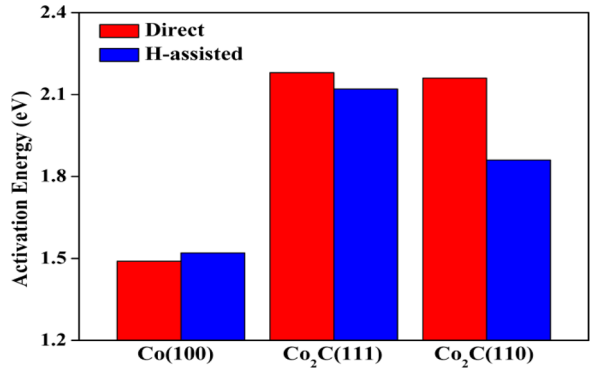

Figure 4. Activation energies (in eV) of direct (red) and H-assisted (blue) CO activation pathways on fcc Co (100), Co-terminated Co_2C (111) and (110) surfaces.

might become favorable. Our calculations on C-terminated $Co_2C(111)$and (110) surfaces show that the CO binding energies are at least −1.86 eV, while the corresponding dissociation barriers for both direct and H-assisted pathways are at least 2.00 eV higher. These show that irrespective to Co_2C surface orientations and termination, its noble-metal-like feature leads it as the efficient active sites for nondissociative adsorption of CO molecules. In this context, we note that we studied thoroughly CO dissociation on both fcc and hcp Co metals in past.[34] Actually, except for close-packed hcp (0001) surfaces, most of the facets exposed in hcp Co were active for CO dissociation, and the corresponding barriers were comparable and even lower than that of fcc Co(100) included in this work. CO dissociative adsorption on Co metal catalysts as well as subsequent C−C coupling for hydrocarbon is therefore clear.

To provide further support on the role of the Co and Co_2C interface for alcohol synthesis, we constructed a simplified model, with a Co strip on the $Co_2C(111)$ surface, on the basis of HRTEM measurement (details in Figure S14 and Table S7). It is found that adsorbed molecular CO on Co_2C can easily insert into the CH_2 intermediate on the Co strip with a barrier of 0.77 eV. The modest value indicates that the interface is indeed facile for alcohol formation. Whereas, on Co_2C (111), the corresponding barrier is 1.48 eV, which is 0.71 eV higher than that of the interface sites. This demonstrates that even hydrocarbon formed on cobalt metal might migrate to cobalt carbide, and the overall contribution to the alcohol formation would be lower, compared with the sites at the Co and Co_2C interface.

In summary, we successfully synthesized stable Co−Co_2C catalysts under the F−T reaction condition. The formation of Co_2C and the interface with the Co metal are essential for the production of the high alpha-alcohols. The selectivity comes from the synergetic effect of the Co−Co_2C catalysts, namely, noble-metal-like Co_2C for CO nondissociative adsorption, and the Co metal for CO dissociative adsorption and subsequent carbon-chain growth. The interface between metal and its carbide phase, free from of precious transition metal, provide the efficient dual sites for synthesizing oxygenates in syngas applications.

DOI: 10.1021/acscatal.5b00791
ACS Catal. 2015, 5, 3620−3624

■ ASSOCIATED CONTENT

Supporting Information

The Supporting Information is available free of charge on the ACS Publications website at DOI: 10.1021/acscatal.5b00791.

Figure S1−14, Table S1−S7 (PDF)

■ AUTHOR INFORMATION

Corresponding Authors

*E-mail: wxli@dicp.ac.cn (W.-X.L.).
*E-mail: dyj@dicp.ac.cn (Y.-J.D.).

Author Contributions

‖Y.-P.P. and J.-X.L. contributed equally.

Notes

The authors declare no competing financial interest.

■ ACKNOWLEDGMENTS

This work received financial support from NSFC (21321002, 21225315, 21173210), MOST(2013CB834603), the Key Research Program and Strategic Priority Research Program of CAS (XDA090301001 and KGZD-EW-T05) and DICP (DICP M201304). The calculations were carried out at National Supercomputing Center in Tianjin, China.

■ REFERENCES

(1) Lundeen, A.; Poe, R. *Encyclopedia of Chemical Processing and Design. 2*; Mc Ketta, J. J., Cunningham, W. A., Eds; Marcel Dekker Inc: New York, 1977.
(2) Freitas, E. R.; Gum, C. R. *Chem. Eng. Prog.* **1979**, *75*, 73−76.
(3) O'Rourke, C. E.; Kavasmaneck, P. R.; Uhl, R. E. *ACS Symp. Ser.* **1981**, *159*, 71−85.
(4) Breit, B. *Acc. Chem. Res.* **2003**, *36*, 264−275.
(5) Dong, W.; Liu, J.; Zhu, H.; Ding, Y.; Pei, Y.; Liu, J.; Du, H.; Jiang, M.; Liu, T.; Su, H.; Li, W. *J. Phys. Chem. C* **2014**, *118*, 19114−19122.
(6) Muramatsu, A.; Tatsumi, T.; Tominaga, H. O. *J. Phys. Chem.* **1992**, *96*, 1334−1340.
(7) Cosultchi, A.; Perez-Luna, M.; Antonio Morales-Serna, J.; Salmon, M. *Catal. Lett.* **2012**, *142*, 368−377.
(8) Ding, Y. J.; Zhu, H. J.; Wang, T.; Jiao, G. P.; Lu, Y. U.S. Patent 7,468,396, 2008.
(9) Ding, Y. J.; Zhu, H. J.; Wang, T.; Jiao, G. P.; Lu, Y. U.S. Patent 7,670,985, 2010
(10) Jiao, G.; Ding, Y.; Zhu, H.; Li, X.; Li, J.; Lin, R.; Dong, W.; Gong, L.; Pei, Y.; Lu, Y. *Appl. Catal., A* **2009**, *364*, 137−142.
(11) Pei, Y. P.; Ding, Y. J.; Zang, J.; Song, X. G.; Dong, W. D.; Zhu, H. J.; Wang, T.; Chen, W. M. *Chin. J. Catal.* **2012**, *33*, 808−812.
(12) Xu, X.; Scholten, J. J. F.; Mausbeck, D. *Appl. Catal., A* **1992**, *82*, 91−109.
(13) Volkova, G.; Yurieva, T.; Plyasova, L.; Naumova, M.; Zaikovskii, V. *J. Mol. Catal. A: Chem.* **2000**, *158*, 389−393.
(14) Lebarbier, V. M.; Mei, D.; Kim, D. H.; Andersen, A.; Male, J. L.; Holladay, J. E.; Rousseau, R.; Wang, Y. *J. Phys. Chem. C* **2011**, *115*, 17440−17451.
(15) Mohandas, J. C.; Gnanamani, M. K.; Jacobs, G.; Ma, W.; Ji, Y.; Khalid, S.; Davis, B. H. *ACS Catal.* **2011**, *1*, 1581−1588.
(16) Ducreux, O.; Lynch, J.; Rebours, B.; Roy, M.; Chaumette, P. *Stud. Surf. Sci. Catal.* **1998**, *119*, 125−130.
(17) Weller, S.; Hofer, L.; Anderson, R. *J. Am. Chem. Soc.* **1948**, *70*, 799−801.
(18) Anderson, R. B.; Hall, W. K.; Krieg, A.; Seligman, B. *J. Am. Chem. Soc.* **1949**, *71*, 183−188.
(19) Bian, G.; Nanba, T.; Koizumi, N.; Yamada, M. *J. Mol. Catal. A: Chem.* **2002**, *178*, 219−228.
(20) Karaca, H.; Hong, J.; Fongarland, P.; Roussel, P.; Griboval-Constant, A.; Lacroix, M.; Hortmann, K.; Safonova, O. V.; Khodakov, A. Y. *Chem. Commun.* **2010**, *46*, 788−790.
(21) Oyama, S. *Catal. Today* **1992**, *15*, 179−200.
(22) Rodriguez, J. A.; Dvorak, J.; Jirsak, T. *J. Phys. Chem. B* **2000**, *104*, 11515−11521.
(23) Nagai, M.; Zahidul, A. M.; Matsuda, K. *Appl. Catal., A* **2006**, *313*, 137−145.
(24) Bahr, H.; Jessen, V. *Ber. Dtsch. Chem. Ges. B* **1930**, *63*, 2226−2237.
(25) Bessell, S. *Appl. Catal., A* **1993**, *96*, 253−268.
(26) Lögdberg, S.; Lualdi, M.; Järås, S.; Walmsley, J. C.; Blekkan, E. A.; Rytter, E.; Holmen, A. *J. Catal.* **2010**, *274*, 84−98.
(27) Anderson, R. B.; Kölbel, H.; Rálek, M. *The Fischer−Tropsch Synthesis*; Academic Press: New York, 1984; Vol. *16*.
(28) Cheng, J.; Hu, P.; Ellis, P.; French, S.; Kelly, G.; Lok, C. M. *J. Phys. Chem. C* **2009**, *113*, 8858−8863.
(29) Cheng, J.; Hu, P.; Ellis, P.; French, S.; Kelly, G.; Lok, C. M. *J. Phys. Chem. C* **2008**, *112*, 6082−6086.
(30) Wang, H.; Zhou, W.; Liu, J.-X.; Si, R.; Sun, G.; Zhong, M.-Q.; Su, H.-Y.; Zhao, H.-B.; Rodriguez, J. A.; Pennycook, S. J.; Idrobo, J.-C.; Li, W.-X.; Kou, Y.; Ma, D. *J. Am. Chem. Soc.* **2013**, *135*, 4149−4158.
(31) Levy, R.; Boudart, M. *Science* **1973**, *181*, 547−549.
(32) Saib, A. M.; Moodley, D. J.; Ciobîcă, I. M.; Hauman, M. M.; Sigwebela, B. H.; Weststrate, C. J.; Niemantsverdriet, J. W.; van de Loosdrecht, J. *Catal. Today* **2010**, *154*, 271−282.
(33) Zhao, Y.-H.; Su, H.-Y.; Sun, K.; Liu, J.; Li, W.-X. *Surf. Sci.* **2012**, *606*, 598−604.
(34) Liu, J.-X.; Su, H.-Y.; Sun, D.-P.; Zhang, B.-Y.; Li, W.-X. *J. Am. Chem. Soc.* **2013**, *135*, 16284−16287.
(35) Huo, C.-F.; Li, Y.-W.; Wang, J.; Jiao, H. *J. Phys. Chem. C* **2008**, *112*, 14108−14116.

DOI: 10.1021/acscatal.5b00791
ACS Catal. 2015, 5, 3620−3624